Proc. Natl. Acad. Sci. USA
Vol. 91, pp. 8782–8786, September 1994
Physiology

On measuring the third dimension of cultured endothelial cells in shear flow

S. Q. Liu, Morris Yen, and Y. C. Fung

Institute for Biomedical Engineering, University of California at San Diego, La Jolla, CA 92093–0412

Contributed by Y. C. Fung, May 13, 1994

ABSTRACT **The stress in the endothelial cells induced by blood flow depends on the waviness of the blood–endothelium interface and the slopes at the junctions of neighboring cells in the direction of flow. The height and slope in the third dimension of the living endothelial cells cannot be measured by ordinary optical and electron microscopy. Here we show that interference microscopy meets the challenge. We measured the geometry of cultured confluent human vascular endothelial cells in a flow, and we found that in a normal section parallel to the flow, the absolute values of the surface slopes at the cell junctions were 0.70 ± 0.02 (SE) and 0.80 ± 0.02 (SE) at the leading and trailing edges of the cells, respectively, in a culture medium of osmolarity 310 mosM with a shear stress of approximately 1 N/m². A reversal of the flow direction led to a reversal of the slope pattern. An increase in medium osmolarity above 310 mosM induced an initial decrease in the slopes followed by a return to normal, whereas a decrease in the osmolarity had a reversed effect. These results, in light of our previous theoretical analyses, show that tensile stress exists in the endothelial cell membrane, and that the mechanism of tension accumulation is a reality. The accumulation is not 100% because the membranes are not smooth at the cell junctions.**

This paper is concerned with the geometric shape of the interface between flowing blood and a blood vessel. The endothelium, which is a confluent layer of endothelial cells, is the biological gateway between the blood and the tissues and organs of the body and is the source of many factors that are critical to health and disease such as atherosclerosis. As sketched in Fig. 1, each endothelial cell adheres on the bottom to the basal lamina, adheres to neighboring cells on the side membranes (sidewalls), and is exposed to the blood flow at the top cell membrane, whose geometry determines the shear stress in the flowing blood that acts on the cell membrane and the tensile stress in the cell membrane. These stresses influence the expression of multiple genes (1) and the endothelial structure and function (2, 3). The well-known Poiseuille formula gives a rough estimate of the shear stress; but more accurate calculations have been given by Dewey and by Yamaguchi *et al.* (4) by using a numerical method and in analogous problems by Fung and Yih (5), and Yin and Fung (6). The stress distribution in the endothelial cell membrane has been analyzed by Fung and Liu (7), who showed that the endothelial cell membrane resists the imposed shear with tension. Fig. 1 shows that for a flow to the left the tension is larger on the right. Now, at the junction of two cells, the membrane tension in cell $i + 1$ on the left can be transmitted partly to the membrane of cell $i + 2$ on the right and partly downward to the basal lamina via the side wall (Fig. 1*A*). However, if the membranes at the junction were smooth as shown in Fig. 1*B*, then all the tension in the membrane of cell $i + 1$ will be transmitted to the membrane of cell $i + 2$. Thus the membrane of cell $i + 2$ must bear not only the shear acting on it directly but also the cumulative tension in the membrane of cell $i + 1$. In either case the mechanism of accumulation can become serious because hundreds of thousands of cells are on line. The reality is closer to Fig. 1*A*. If the *in vivo* blood shear is 1 N/m², then the tension in the cell membrane can be 10^4 N/m² or larger, which causes a shear stress of 5×10^3 N/m² or larger acting on planes inclined at 45° to the direction of tension. If integrins or ion channels were lined up with these inclined planes, they could, theoretically, be sensitive to the large shear stress. Thus the significance is seen.

In the past, the significance of the membrane geometry of the endothelial cells was unknown, and there is no known method for its determination. An atomic force microscope may be applied (8), but it is difficult to use it in a flowing fluid. Electron microscopy requires tissue fixation and dehydration, which can induce geometric distortion. Facing these difficulties, we recalled our early work on the determination of the thickness profile of erythrocytes by using a Mach–Zender interference microscope (9–13), which yielded data with a resolution of 0.02 μm based on physical optics. Hence we hypothesized that it might yield the endothelium profile.

MATERIALS AND METHODS

A human vascular endothelial cell line was generously provided by C.-J. S. Edgell (University of North Carolina, Chapel Hill). The cells were cultured with Dulbecco's modified Eagle's medium supplemented with 15% fetal bovine serum (HyClone), HAT (100 μM hypoxanthine/0.4 μM aminopterin/16 μM thymidine), L-glutamine (0.48 mg/ml), penicillin (50 units/ml), and streptomycin (0.05 mg/ml) (14). The culture medium and supplements, except bovine serum, were purchased from Sigma. Once confluent, the cells were harvested by trypsin digestion, diluted 1:8, and plated onto gelatin-coated microscope coverslips. A confluent layer of cells was formed in 3–5 days after plating. The coverslip with a confluent cell layer was mounted into a cell chamber for microscopic observation. The cell chamber was constructed by stacking together a glass microscope coverslip with cultured cells on one side, an inert plastic gasket 0.36 mm in thickness with a rectangular opening at the center (3.6 × 36 mm) which served as a flow channel, and a glass microscope slide as the base. Two small holes 34 mm apart were drilled in the microscope coverslip to serve as the inlet and outlet of the flow of the culture medium. The cultured cells on the microscope coverslip face the fluid flow. Two stainless steel covers (with a central hole in each for light transmission) were placed above and below the cell chamber to serve as a frame.

During an experiment, the circulatory culture medium was bubbled with a filtered gas mixture of 95% O_2/5% CO_2, maintained at 37°C in a reservoir with a warm water bath, and in the cell chamber by a feedback-controlled electric heating pad placed on the top of the chamber. Unless mentioned otherwise, the circulating medium had an osmolarity of 310

The publication costs of this article were defrayed in part by page charge payment. This article must therefore be hereby marked "*advertisement*" in accordance with 18 U.S.C. §1734 solely to indicate this fact.

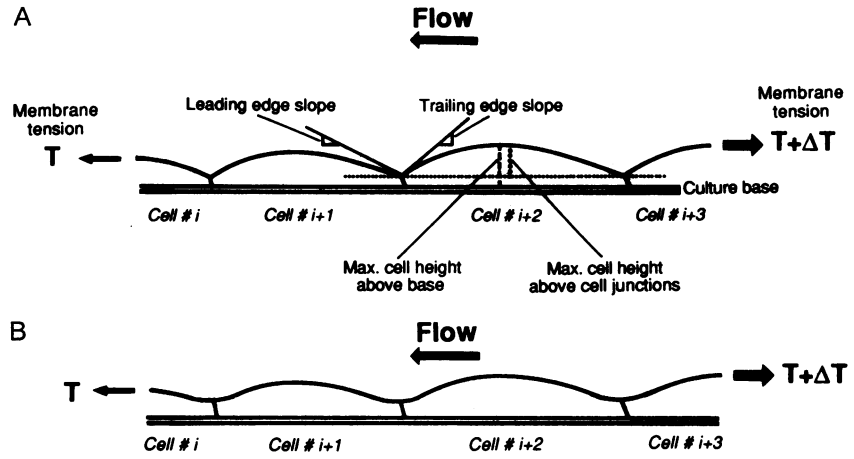

FIG. 1. Blood shear induces tension in endothelial cell membranes. There are two possible shapes of the cross section of an endothelium. (*A*) The neighboring cell membranes intersect at a sharp angle. (*B*) The neighbors meet smoothly. The way of tension transmission is different in these two cases. See text.

mosM, a pressure head of 3 cm H_2O, and a flow rate of ≈3 ml/min, at a shear stress of the order of 1 N/m^2.

A Leitz interference microscope with a pair of ×85 oil-immersion objectives and a monochromatic mercury light source was provided by Shu Chien (University of California, San Diego). The principle of interference microscopy is given in refs. 9 and 15. Briefly, a light beam is split into two beams, which separately pass through two identical lens systems in the interference microscope with a flow chamber containing the cells and culture medium in the path of one beam, and another identical chamber containing the culture medium alone in the path of the other beam. When the two beams of light are finally recombined, they interfere with each other and produce a pattern of alternate bright and dark fringes. The bright fringes are where the two waves are in phase. The dark fringes are where the two waves are 180° out of phase. When the cells are absent, the interference fringes are straight lines. Deviation from a straight line is caused by a light beam passing through cells inducing a phase shift because the velocity of light in the cell is different from that in the medium. The phase shift, Φ, is linearly proportional to the product of the thickness of the cell, D, and the difference of the index of refraction of the cell, η_c, and that of the culture medium, η_m. If λ denotes the wavelength of the light (0.546 μm in our experiment), then the phase shift is given by the formula (9)

$$\Phi = (2\pi/\lambda)(\eta_c - \eta_m)D. \quad [1]$$

To measure the index of refraction of the cells, we used a matching-solution technique introduced by Barer and Joseph (15). Under the interference microscope, the fringes passing through several endothelial cells were observed. Bovine serum albumin was added into the culture medium gradually until the curvature of the fringes on the cells disappeared, signaling the vanishing of the phase shift, and the identity of the refractive indices of the cells and the albumin/medium mixture. The index of refraction of the culture medium and albumin/medium mixture was then measured according to Snell's law. We found $\eta_c = 1.411 \pm 0.010$ ($n = 6$) for the cultured endothelial cells and $\eta_m = 1.344 \pm 0.014$ ($n = 6$) for the medium without albumin.

To obtain the geometry of individual endothelial cells in a confluent monolayer, cells were selected randomly and ordinary and interference images were recorded, observed, and analyzed. A typical example is shown in Fig. 2. To determine

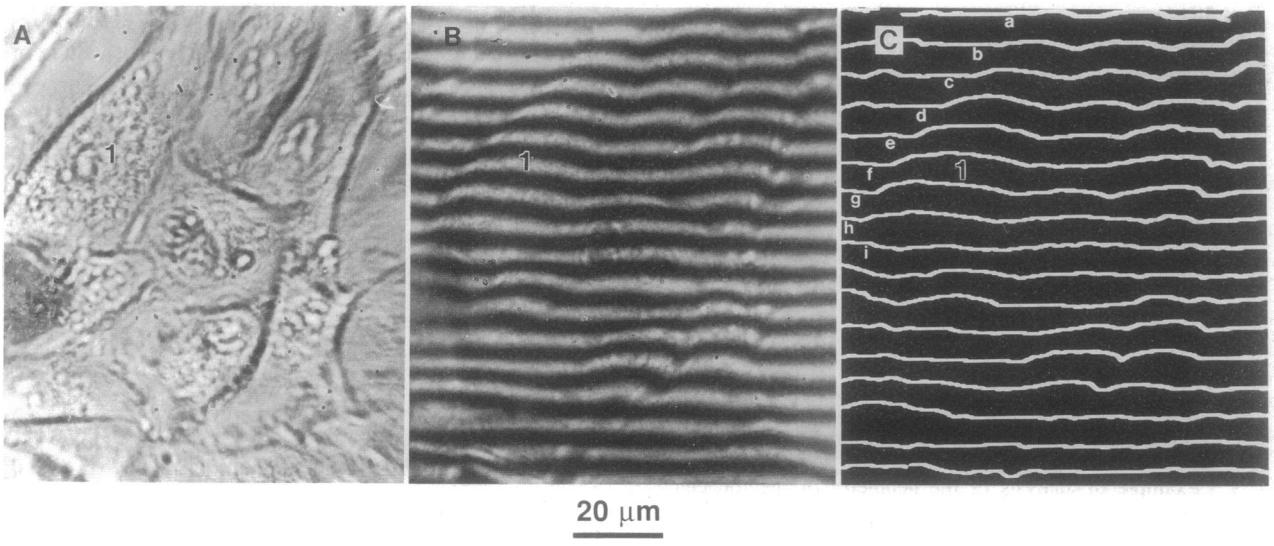

FIG. 2. Microscopic images of cultured endothelial cells in a flow chamber at a flow rate that generates a shear stress of about 1 N/m^2. (*A*) Ordinary plane image. (*B*) Image of the same cells as shown in *A* under an interference microscope. (*C*) Image of *B* enhanced by using an Optimas image processing system. Medium osmolarity: 310 mosM. Medium flow direction: right to left.

the effect of shear flow on the geometry of the endothelial cell membrane, a flow with a shear stress of ≈1 N/m² was imposed for 60 min. The cell membrane geometry was continuously observed, recorded, and analyzed. The flow direction was then reversed, and the same experimental protocol was repeated. Finally, to study the effect of osmolarity, the cells were exposed to a medium of 310 mosM and a shear flow at a shear stress of 1 N/m² for 1 hr, observed, and recorded. The medium osmolarity was then changed in several steps in the following order: (*i*) from 310 to 360 mosM by adding NaCl, (*ii*) from 360 to 310 mosM, and (*iii*) from 310 to 260 mosM by adding distilled water. The cells were observed for 1 hr after each step, recorded, and measured. The medium osmolarity was determined by using the freezing point method with an Advanced DigiMatic model 3D II osmometer (Advanced Instruments, Needham Heights, MA).

The recorded interference images of endothelial cells were enhanced with an Optimas Image Analysis system (Bioscan, Edmonds, WA), digitized, converted into surface height by Eq. 1, then plotted and fitted by a cubic spline equation (16). An example is given in Fig. 2, which shows an ordinary image (*A*); an interference image of the same cells with undisturbed fringes parallel to the streamlines of flow (*B*); and an image enhanced by using the Optimas software (*C*). The first and second derivatives (slope and curvature, respectively) were calculated. Fig. 3*A* shows a cubic spline fitted curve from fringe b shown in Fig. 2*C*. It represents a cross section of the cells in a plane normal to the base of the endothelium and parallel to the flow. We shall call this curve a *normal intercept*. In each normal intercept there is a *maximal height above the base*, which is called the *maximal thickness of the cross section*. To measure the maximal thickness we scraped off the cells in a selected area to reveal the base. A fringe passing through the base in this area and cells beyond its border then reveals the height of these cells above the base. Fig. 3*B* shows the slope and curvature of the normal intercept shown in Fig. 3*A*. In an interference image, the location of the cell junction is defined as the point with a maximal curvature and a zero slope. The cell membrane slope at a junction changes rapidly from a maximal negative, to zero, then to a maximal positive value in a distance of about 1 μm. These

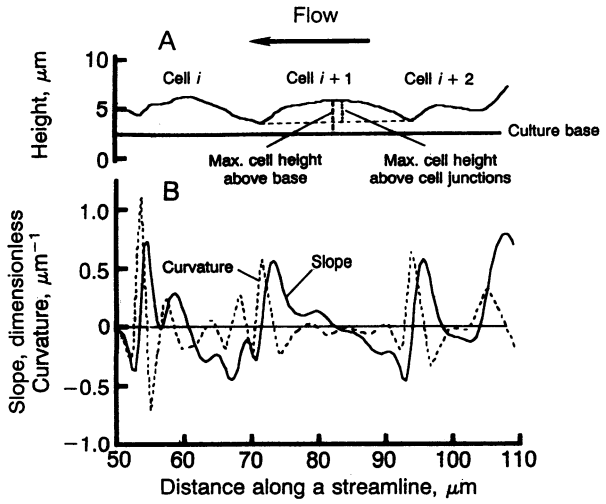

FIG. 3. Example of analysis of the geometry of the top cell membranes of the endothelial cells as a continuum. (*A*) Cubic spline fitted curve of the top cell membranes of three consecutive cells. This curve was converted from interference fringe b in Fig. 2*C*. The cells are numbered *i*, *i* + 1, *i* + 2, etc. (*B*) Slope (solid line) and curvature (broken line) of the top cell membrane shown in *A*, computed by using a cubic spline curve fitting equation. See text for explanations.

maximal slopes at the vicinity of the junctions were measured.

Statistical analyses were made. Raw data histograms are presented. Changes in the geometric parameters under the influence of shear stress and medium osmolarity are presented with respect to time.

RESULTS

Surface Geometry of Single Cells. The maximal surface height above the cell junctions and the leading- and trailing-edge slopes of the indicated normal intercepts of cell no. 1 in Fig. 2 in planes parallel to the streamlines of flow are shown in Fig. 4. This cell is elongated, with a major axis oriented at an angle of about 60° from the flow direction.

Average Geometric Parameters. Fig. 5 shows the histograms of the trailing-edge slopes of the top membrane of 126 cells. Fig. 6 shows the maximal cell height above the base of 72 cells. These parameters were measured from one interference fringe located at the middle region of each selected cell. The values of the leading- and trailing-edge slopes were −0.70 ± 0.02 (SE) and 0.80 ± 0.02 (SE), respectively. The absolute value of the slope at the leading edge of the cells was significantly smaller than that at the trailing edge ($P < 0.001$). The maximal height above the cell junctions of the top cell membranes was 2.50 ± 0.05 (SE) μm, and the maximal height of the cells above the base was 3.46 ± 0.05 (SE) μm.

Effect of Shear Flow. Fig. 7 shows the changes in the leading- and trailing-edge slopes of the top endothelial cell membrane in response to shear flow. It was found that the leading-edge slopes of the cells were gradually decreased with time in shear flow, whereas the trailing-edge slopes of the cells gradually increased. A reversal of the flow direction in the cell chamber induced a reversed change in the cell slopes.

Effect of Osmolarity. Fig. 8*A* shows changes in the leading- and trailing-edge slopes and the maximal height of the top cell membrane above the cell junctions in response to several step changes in medium osmolarity. The slopes remained relatively stable in a culture medium with an osmolarity of 310 mosM. When the osmolarity was suddenly increased from 310 to 360 mosM by adding NaCl, the absolute value of the leading- and trailing-edge slopes decreased rapidly in the first several minutes by about 35% and 34% of the baseline values, respectively, then returned gradually to the control levels in about 25 min and increased slightly afterwards. When the medium osmolarity was changed from 360 mosM back to 310 mosM by adding distilled water, the absolute values of the

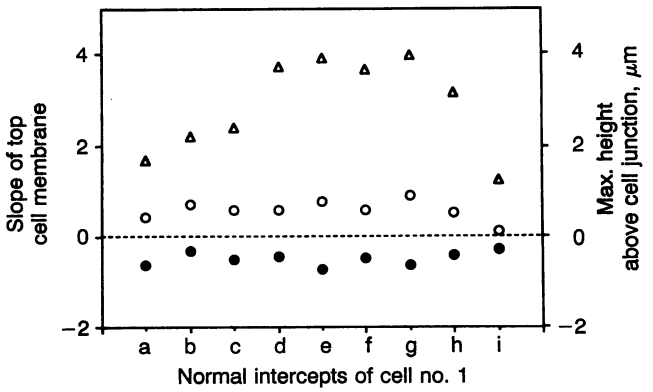

FIG. 4. Typical example of the distribution of the leading-edge and trailing-edge slopes and the maximal height of an endothelial cell above the cell junction, measured from a total number of 9 interference fringes labeled as a, b, c, . . . i passing through the cell no. 1 shown in Fig. 2*C*. ●, Leading-edge slope; ○, trailing-edge slope; △, maximal cell height.

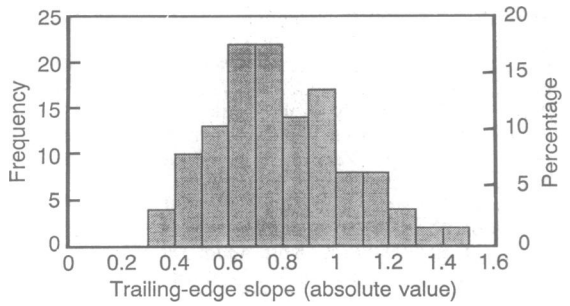

FIG. 5. Histogram of the trailing-edge slope of the endothelial cells. Osmolarity: 310 mosM.

leading- and trailing-edge slopes increased in about 5 min by 27% and 33% of the baseline values, respectively, then returned gradually to the control level in about 20 min and further decreased somewhat afterwards. When the osmolarity of the culture medium was reduced from 310 to 260 mosM, the changes in slopes of the endothelial cells were similar to those in response to an osmolarity change from 360 to 310 mosM. The progressive change of the maximal cell height above the junctions in response to alterations in the medium osmolarity is similar to that of the trailing-edge slope.

DISCUSSION

Interference microscopy supplies the needed information about the geometry of the top cell membrane of cultured living cells in a flow field. By comparing the leading- and trailing-edge slopes of the endothelial cell membrane, it was found that the absolute value of the leading-edge slope was smaller than that of the trailing edge. A reversal of the flow direction induced a reversal of the slopes at these junctions. These results suggest that the shear stress acting on the endothelial cells is responsible for the progressive change in the slopes of the top cell membrane.

The slope and curvature of the cell membrane indicate that the static pressure inside the endothelial cell is higher than that in the flowing fluid and that tension exists in the cell membrane. This is because, according to the Laplace formula, tension times curvature equals the static pressure difference across a membrane. If the cytoskeletal fibers exert tension inside the cell, as postulated by the tensegrity model of Ingber (17, 18) and vouched by the observations of Nerem and coworkers (19, 20), then the term "static pressure" in the preceding sentence should mean the hydrostatic pressure of the fluid inside the cell minus the tensile stress exerted by the cytoskeletal fibers on the inner surface of the top cell membrane. With this change in the Laplace formula, we see that the outward bulging implies an excess of internal hydrostatic pressure over the cytoskeleton stress, and the existence of cell membrane tension. As analyzed in ref. 7, the larger the slopes of the cell membranes at the junctions, the smaller may be the transmission of tension from one cell to the next, and the less the accumulation of tensile stress due to flow. The smaller the slopes, or the smoother the cell membrane at the junctions, the larger the tension accumulation due to a long line of cells. The slopes we found are relatively small, indicating that the membrane tensile stress accumulation mechanism must be carefully studied in the future.

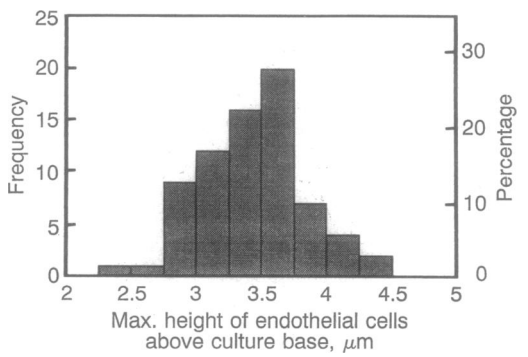

FIG. 6. Histogram of the cell height above the base of the endothelium. Osmolarity: 310 mosM.

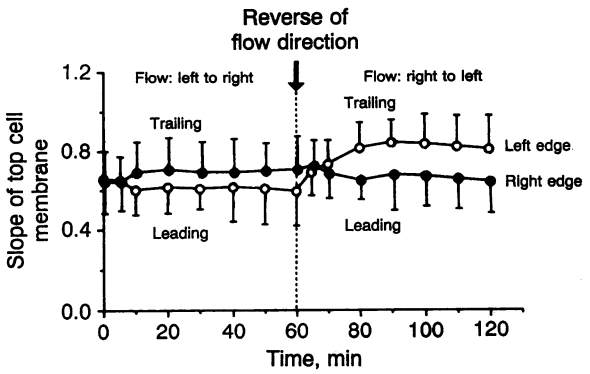

FIG. 7. Effect of shear flow on the leading-edge and trailing-edge slopes of the endothelial cells. Points are mean ± SD.

Osmolarity is one of the factors regulating the ion and water transport across cell membranes and the cell geometry (21–24). Fig. 8 shows that a step increase of osmotic pressure of the flowing medium reduces the cell height, the membrane slope, and the static pressure inside the cell. But in time a stable cell volume is reached. A step decrease of the external osmotic pressure has an opposite effect. Thus the endothelial cells show a high level of volume regulation. However, since the stretch-sensitive ion channels are influenced by shear and tensile stresses in the cell membrane (25–27), the effect of osmolarity at higher tensile membrane stress should be

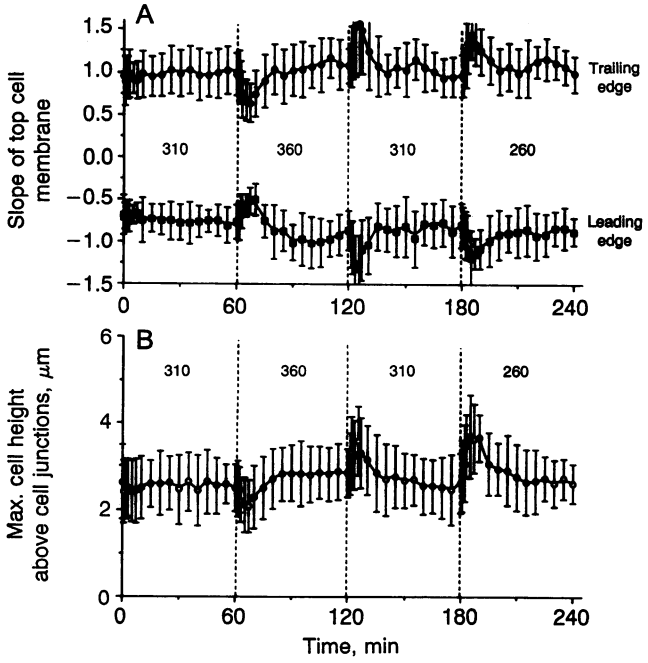

FIG. 8. (*A*) Time course of changes in the leading- and trailing-edge slopes of endothelial cells in response to several step changes in medium osmolarity (given in mosM). (*B*) Time course of changes in the maximal surface height of the endothelial cells in response to several step changes in medium osmolarity. Results are mean ± SD.

studied. Interference microscopy may also help in the study of the effects of stretch on growth (28–31) and biochemical processes and gene expression (32–34).

The cell contents are not uniform. Could some of the features seen in Fig. 3*B* be due to a nonuniform refractive index in a cell? The answer is no, because we were able to obtain straight interference fringes passing through endothelial cells when an appropriate amount of albumin was added into the medium surrounding the cells, indicating a uniform index of refraction in the cell, since the medium and the chamber height were uniform.

We thank Dr. Shu Chien for providing us with the interference microscope, Dr. C. J. S. Edgell for sending us the EA.hy 926 endothelial cell line, Dr. John Shyy and Ms. Catherine Galbraith for help in cell culture, and Dr. J. B. Zhou for help in data analysis. This research is supported by National Heart, Lung and Blood Institute Grants HL-26647 and HL-43026 and by National Science Foundation Grant BCS 89-17576.

1. Resnick, N., Collins, T., Atkinson, W., Bonthron, D. T., Dewey, C. F., Jr., & Gimbrone, M. A., Jr. (1993) *Proc. Natl. Acad. Sci. USA* **90,** 4591–4595.
2. Dewey, D. F., Jr., Bussolari, S. R., Gimbrone, M. A., Jr., & Davies, P. F. (1981) *J. Biomech. Eng.* **103,** 177–185.
3. Davies, P. F. & Tripathi, S. C. (1993) *Circ. Res.* **72,** 239–245.
4. Yamaguchi, T., Hoshiai, K., Okino, H., Sakurai, A., Hanai, S., Masuda, M. & Fujiwara, K. (1993) *Proc. Bioeng. Conf.* **24,** 167 (abstr.).
5. Fung, Y. C. & Yih, C. S. (1968) *J. Appl. Mech.* **35,** 669–675.
6. Yin, F. C. P. & Fung, Y. C. (1971) *J. Fluid Mech.* **47,** 93–112.
7. Fung, Y. C. & Liu, S. Q. (1993) *J. Biomech. Eng.* **115,** 1–12.
8. Barbee, K. A., Davies, P. F. & Lal, P. (1994) *Circ. Res.* **74,** 163–171.
9. Evans, E. & Fung, Y. C. (1972) *Microvasc. Res.* **4,** 335–347.
10. Tsang, W. C. O. (1975) M.S. thesis (Univ. of California at San Diego, La Jolla, CA).
11. Fung, Y. C., Tsang, W. C. O. & Patitucci, P. (1981) *Biorheology* **18,** 369–385.
12. Chen, P. & Fung, Y. C. (1973) *Microvasc. Res.* **6,** 32–43.
13. Fung, Y. C. (1993) *Biomechanics: Mechanical Properties of Living Tissues* (Springer, New York), 2nd Ed.
14. Emeis, J. J. & Edgell, C.-J. S. (1988) *Blood* **71,** 1669–1675.
15. Barer, R. & Joseph, S. (1955) *Q. J. Microsc. Sci.* **96,** 1–27.
16. Press, W. H., Flannery, B. P., Teukolsky, S. A. & Vetterling, W. T. (1989) *Numerical Recipes: The Art of Scientific Computing (FORTRAN Version)* (Cambridge Univ. Press, Cambridge, U.K.), pp. 86–88.
17. Ingber, D. E., Madri, J. A. & Folkman, J. (1987) *In Vitro Cell. Dev. Biol.* **23,** 387–394.
18. Ingber, D. E. (1990) *Proc. Natl. Acad. Sci. USA* **87,** 3579–3583.
19. Helmlinger, G., Geiger, R. V., Schreck, S. & Nerem, R. M. (1991) *J. Biomech. Eng.* **113,** 123–131.
20. Nerem, R. M. & Girard, P. R. (1990) *Toxicol. Pathol.* **18,** 572–582.
21. Hoffmann, E. K. (1987) *Curr. Top. Membr. Transp.* **30,** 125–180.
22. Lauf, P. K., Bauer, J., Adragna, N. C., Fujise, H., Zade-Oppen, A. M. M., Ryu, K. H. & Delpire, E. (1992) *Am. J. Physiol.* **263,** C917–C932.
23. Eveloff, J. L. & Warnock, D. G. (1987) *Am. J. Physiol.* **252,** F1–F10.
24. Christensen, O. (1987) *Nature (London)* **330,** 66–68.
25. Lansman, J. B., Hallam, T. J. & Rink, T. J. (1987) *Nature (London)* **325,** 811–813.
26. Sachs, F. (1989) in *Cell Shape: Determinants, Regulation, and Regulatory Role,* eds. Stein, W. D. & Bronner, F. (Academic, San Diego), pp. 63–92.
27. Morris, C. E. (1990) *J. Membr. Biol.* **112,** 93–107.
28. Lau, K. R., Hudson, R. L. & Schultz, S. G. (1984) *Proc. Natl. Acad. Sci. USA* **81,** 3591–3594.
29. Mann, D. L., Kent, R. L. & Cooper, G., IV (1989) *Circ. Res.* **64,** 1079–1090.
30. Fung, Y. C. (1984) *Biodynamics: Circulation* (Springer, New York).
31. Leung, D. Y., Glagov, S. & Mathews, M. (1976) *Science* **191,** 475–477.
32. Watson, P. A. (1990) *J. Biol. Chem.* **265,** 6569–6575.
33. Watson, P. A. (1991) *FASEB J.* **5,** 2013–2019.
34. Komuro, I., Katoh, Y., Kaida, T., Shibazaka, Y., Kurabayashi, M., Takaku, F., Hoh, E. & Yazaka, Y. (1991) *J. Biol. Chem.* **266,** 1265–1268.